ACS APPLIED MATERIALS & INTERFACES

Research Article

www.acsami.org

Nanosomal Microassemblies for Highly Efficient and Safe Delivery of Therapeutic Enzymes

Huarong Xiong,[†,#] Yunli Zhou,[†,#] Qixin Zhou,[†,#] Dan He,[†,#] Shengli Wan,[†,#] Qunyou Tan,[‡] Mi Zhang,[†] Xue Deng,[†] and Jingqing Zhang*[,†]

[†]Medicine Engineering Research Center, Chongqing Medical University, Chongqing 400016, China

[‡]Department of Thoracic Surgery, Institute of Surgery Research, Daping Hospital, Third Military Medical University, Chongqing 400042, China

Supporting Information

ABSTRACT: Enzyme therapy has unique advantages over traditional chemotherapies for the treatment of hyperuricemia, but overcoming the delivery obstacles of therapeutic enzymes is still a significant challenge. Here, we report a novel and superior system to effectively and safely deliver therapeutic enzymes. Nanosomal microassemblies loaded with uricase (NSU-MAs) are assembled with many individual nanosomes. Each nanosome contains uricase within the alkaline environment, which is beneficial for its catalytic reactions and keeps the uricase separate from the bloodstream to retain its high activity. Compared to free uricase, NSU-MAs exhibited much higher catalytic activity under physiological conditions and when subjected to different temperatures, pH values and trypsin. NSU-MAs displayed increased circulation time, improved bioavailability, and enhanced uric acid-lowering efficacy, while decreasing the immunogenicity. We also described the possible favorable conformational changes occurring in NSU-MAs that result in favorable outcomes. Thus, nanosomal microassemblies could serve as a valuable tool in constructing delivery systems for therapeutic enzymes that treat various diseases.

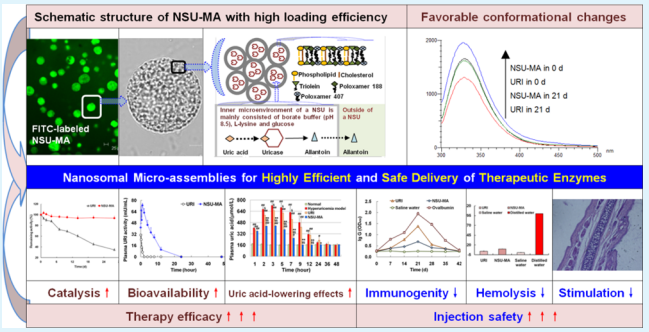

KEYWORDS: *nanosomal microassembly, therapeutic enzyme, delivery system, microenvironment, hyperuricemia treatment*

INTRODUCTION

The prevalence of hyperuricemia among Chinese adults in 2009−2010 was 8.4%.[1] There has been an increasing worldwide prevalence of diseases associated with hyperuricemia. These associated diseases include but are not limited to gout, incident hypertension and cardiometabolic disease.[2] Enzyme therapies are more effective than traditional chemotherapies in some aspects. For example, uricase (URI) dissolves and eliminates existing uric acid, whereas allopurinol and febuxostat do not. Although URI has been used to treat hyperuricemia for over 40 years,[3] its clinical application has been hampered by drawbacks such as low stability, low catalytic activity and high immunogenicity, which result in inadequate therapy and undesirable side effects.[4] Therefore, recombinant URI was developed to improve enzymatic activity,[5,6] and polyethylene glycol (PEG) was bound to the recombinant URI to prolong its circulation time.[7,8] Both rasburicase (recombinant URI) and pegloticase (PEGylated recombinant URI) have already been approved for clinical applications. It should be noted that when prolonging the plasma half-life time, pegloticase reduced the catalyzed activity of recombinant URI. Furthermore, both of these medications have high immunogenicities.[9] Therefore, it is necessary to develop superior URI delivery systems with enhanced and sustained catalytic activities while decreasing the immunogenicity when administered in vivo.

Herein, we report the use of URI-encapsulating alkaline nanosomal microassemblies (NSU-MAs), which simultaneously possess the required attributes for improved URI delivery: increased stability, enhanced catalytic activity, sustained therapeutic effects and lowered immunogenicity. Each alkaline nanosome encapsulates a specific number of URI molecules. The semipermeable lipid membrane of each nanosome contains URI inside an alkaline environment consisting of borax buffers at pH 8.5 (the optimal pH for URI activity) and separates URI from the external bloodstream to increase its stability and long-term catalytic activity, similar to our recent reports with the URI liposome.[10,11] NSU-MAs are assembled with many individual nanosomes, as shown in Figure 1A and 1B; thus, they have a higher URI-loading efficiency, as well as markedly enhanced and sustained catalytic activities, compared to free URI. Furthermore, because the large-molecule protein enzyme URI (tetramers of 35 kDa subunits) has been encapsulated inside the nanosomes that are made of

Received: June 30, 2015
Accepted: August 25, 2015
Published: August 25, 2015

DOI: 10.1021/acsami.5b05758
ACS Appl. Mater. Interfaces 2015, 7, 20255−20263

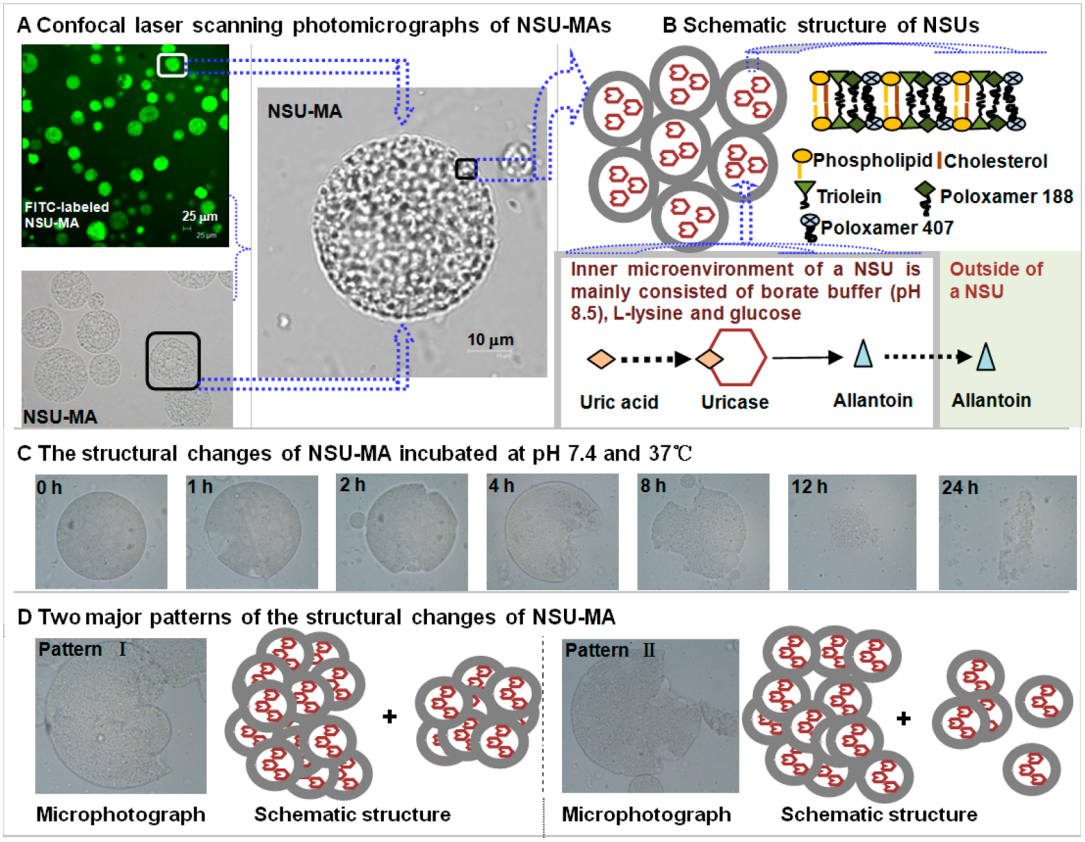

Figure 1. Schematic illustration of the structural changes of NSU-MAs. NSU-MAs are assembled with many individual nanosomes encapsulating URI molecules. (A) Confocal laser scanning photomicrographs of NSU-MAs. (B) Schematic structure of NSUs. (C) The structural changes of NSU-MA incubated at pH 7.4 and 37 °C. (D) Two major patterns of the structural changes of NSU-MAs.

biodegradable pharmaceutical excipients, which are generally recognized as safe (GRAS) and approved by the Food and Drug Administration of many countries, NSU-MAs are considered to have low immunogenicity.

EXPERIMENTAL SECTION

Materials and Instrumentation. Uricase (URI) from the *Candida utiliz* species (activity of 4.9 units/mg powder at 25 °C), uric acid, and fluorescein isothiocyanate (FITC) were obtained from Sigma-Aldrich (St. Louis, MO, USA). Phospholipids (soybean lecithin, Lipoid S 100) were obtained from Lipoid GmbH (Ludwigshafen, Germany). Cholesterol was obtained from Tianma Fine Chemical Plant (Guangzhou, China). Triolein was obtained from Sinopharm Chemical Reagent Co. Ltd. (Shanghai, China). Poloxamer 188 and 407 were obtained from Nanjing Well Biochemical Co. Ltd. (Nanjing, China). L-lysine was obtained from Beijing Dingguo Changsheng Biotechnology Co. Ltd. (Beijing, China). Glucose was obtained from Chongqing Boyi Chemical Reagent Co. Ltd. (Chongqing, China). Borax was obtained from Qiangshun Chemical Co., LTD (Shanghai, China). Boric acid was obtained from Chuandong Chemical (Group) Co., Ltd. (Chongqing, China). Coomassie blue G-250 was obtained from Sinopharm Chemical Reagent Co. LTD (Shanghai, China). Methanol and acetonitrile, all of HPLC grade, were purchased from American TEDIA (Fairfield, OH, USA). HPLC-grade water was purified by a Milli-Q system equipped with cellulose nitrate membrane filters (47 mm × 0.2 mm, Whatman, Maidstone, UK). All other reagents and solvents used in the study were of analytical grade. Male Sprague–Dawley (SD) rats (200 ± 20 g) were supplied by the Laboratory Animal Center at Chongqing Medical University (Chongqing, China). All of the animals were acclimatized at a temperature of 25 ± 3 °C and a relative humidity of 70 ± 5% under natural light/dark conditions for 1 week before dosing. All of the animal experiments were performed in accordance with the protocol approved by the Laboratory Animal Committee at Chongqing Medical University.

Preparation of NSU-MAs. Phospholipids (60.0 mg), cholesterol (46.2 mg), and triolein (66.2 mg) were dissolved in 3 mL of diethyl ether, and the resulting solution was added to 3 mL of 50 mmol/L borate buffer at pH 8.5 (containing 3% glucose, 5% poloxamer 188, 22.5% poloxamer 407 and 2 mg URI). The solution was then vortexed for 8–10 min to obtain a milky dispersion. Next, 3 mL of the emulsion was quickly injected into 10 mL of 50 mmol/L borate buffer at pH 8.5 (containing 4% glucose and 40% mmol/L L-lysine), and the mixture was blended in a homogenizer at 6000 rpm for 24 s to obtain an emulsion. The emulsion was rotated for 15 min to remove the organic solvent in order to form uniform NSU-MAs.

Principal Characteristics of NSU-MAs. The zeta potentials of the NSU-MAs were determined by dynamic light scattering (Zeta-Sizer Nano ZS90 instrument, Malven Instruments Ltd., UK). The average particle size of the NSU-MAs was obtained by measuring the diameters of five hundred particles.[12,13] The sample was prepared by diluting the final preparation described above with a 9 × volume of corresponding buffer.

The morphologies of the NSU-MAs were observed using a laser microdissection system (Leica AS LMD, Wetzlar, Germany) with either a laser light (excitation = 497 nm) or with natural light.

The entrapment efficiency of the NSU-MAs was determined by dividing the amount of the contained enzyme by the total amount of enzyme in the vesicle system.[4] The entrapped enzyme was separated from its vesicle using a gel exclusion chromatography method (with a 15 mm × 400 mm Sephadex G-200 column). Enzyme content was determined using Coomassie blue staining.[14]

Interaction between URI and NSU-MA Membrane. The interaction of URI with the NSU-MA was determined according to the FITC fluorescence method as previously reported.[4] Briefly, URI

DOI: 10.1021/acsami.5b05758
ACS Appl. Mater. Interfaces 2015, 7, 20255–20263

(100 μg/mL) and the blank NSU-MAs were separately mixed with FITC at a volume ratio of 49:1. After separately incubating these mixtures for 5 min in the dark, the solutions were excited at 480 nm, and the emission fluorescence intensities were recorded between 500 and 600 nm using a fluorescence spectrophotometer (F-2500, Shimadzu). The effect of URI alone was examined by incubating URI with empty NSU-MAs for 1 h at 25 °C before adding the FITC solution.

Effects of Temperature on the Activity. The optimum temperature of NSU-MAs was investigated in the temperature range of of 20−70 °C. The URI activity was determined according to a previous study.[11] One U/mL of URI was defined as the amount of URI able to oxidize 1 μmol/L of uric acid to allantoin per minute at 25 °C.

The hypothermal (4 °C) stability was investigated by incubating NSU-MAs at 4 °C for 28 d. The remaining activities were determined at predetermined times. The electrical conductivities of NSU-MAs (100 μg/mL) and free URI (in 50 mmol/L of pH 8.5 borax buffer) were determined at 25 °C by using an electric conductivity analyzer (DDS-307A; Shanghai Yidian Scientific Instrument Co., Ltd., Shanghai, China). Fluorescence changes of URI were determined using a fluorescence spectrophotometer (F-2500, Shimadzu).[15] The emission fluorescence intensity from 300 to 500 nm was recorded upon excitation at 280 nm. Chloroform was added into the NSU-MAs at a volume ratio of 1:2, and then the mixture was centrifuged at 3000 rpm for 5 min; the supernatant was removed and tested as described above. The change in the ultraviolet absorbance of URI was determined using a spectrophotometer (UV-2600, Shimadzu). The NSU-MAs were treated with chloroform and tested as described above. Polyacrylamide gel electrophoresis (PAGE) was performed as previously described.[5] Briefly, equal amounts of free URI and NSU-MAs were spotted and subjected to electrophoresis (Bio-Rad Laboratories, Hercules, CA, USA). After running to completion, the gel was stained with Coomassie brilliant blue R-250 dye solution for 20 min and then destained with a destaining solution (methanol:acetic acid:distilled water at a volume ratio of 1:1:8) for 2 d. The sodium dodecyl sulfate-polyacrylamide gel electrophoresis (SDS-PAGE) was performed in a similar manner. The differences were as follows: samples were heated in a boiling water bath for 5 min before they were spotted, and 10% SDS was added to both the separation gel and spacer gel.

The thermal stability was measured by incubating NSU-MAs at 55 °C for 5 h. The remaining activities were determined at predetermined times. Changes in the fluorescence profile of URI induced by heat treatment was determined according to a modified FITC fluorescence method.[4] Briefly, UCU and NSU-MAs were separately incubated at either 55 or 25 °C for 3 h. Then, free URI was mixed with FITC and prepared as described above followed by measurement of the emission fluorescence intensity from 500 to 600 nm using an excitation wavelength of 480 nm. The NSU-MAs alone were treated with chloroform and tested as a control.

Effects of Acidity-Alkalinity on the Activity. The optimum acidity-alkalinity (pH) of the NSU-MA was investigated in the pH range of 7.0−9.5. The URI activity was determined based on a previous study.[11]

The effects of acidity-alkalinity on the NSU-MAs were determined as follows: Free URI (or NSU-MAs) was incubated with its corresponding buffer in a pH range from 5.0 to 9.5 at 40 °C for 40 min, and the remaining UCU activity was determined at 25 °C.

Effects of Proteolytic Enzyme on the Activity. The effects of trypsin on the NSU-MAs were determined as follows: The NSU-MAs were treated with trypsin at 37 °C to final concentrations of 100 μg/mL for both compounds. Aliquots were taken at predetermined times and assayed.

Kinetic Features of NSU-MA. The in vitro kinetic parameters of URI were determined by catalyzing the oxidation of uric acid solutions at different concentrations (10, 20, 30, 40, and 50 μmol/L) at 25 °C.[14] The reaction medium contained 100 μg/mL of free URI or NSU-MAs. The enzyme kinetic parameters were calculated using the Lineweaver−Burk eq eq 1.

$$\frac{1}{V} = \frac{K_{im}}{V_{max}} \cdot \frac{1}{[S]} + \frac{1}{V_{max}} \quad (1)$$

where V is the reaction velocity, $[S]$ is the substrate (uric acid) concentration, K_m is the Michaelis constant, and V_{max} is the maximum velocity.

All of the experiments were approved by the Institutional Animal Care and Use Committee at Chongqing Medical University. Thirty SD rats (200 ± 20 g) were intravenously administered with either free URI or NSU-MAs at the same URI dose of 2000 mU/kg. Blood samples were obtained from the posterior orbital venous plexus at predetermined times and centrifuged for 10 min at 3000 rpm for further analysis. The plasma URI activity was measured as previously described.[11] The pharmacokinetic parameters and bioequivalence evaluation were calculated using Drug and Statistics software (DAS, version 2.1.1, Mathematical Pharmacology Professional Committee of China, Shanghai, China).

Uric Acid-Lowering Effects of NSU-MA in Hyperuricemia Rats. All of the experiments were approved by the Institutional Animal Care and Use Committee at Chongqing Medical University. A rat model of hyperuricemia was generated as previously described.[11] Briefly, male rats (200 ± 20 g) were administered hypoxanthine orally and oxonic acid potassium salt subcutaneously.

The uric acid-lowering effects of NSU-MAs via intravenous administration were arranged as follows: group 1 (six rats per group) was a normal rat group (negative control group); group 2 was a hyperuricemia rat model group without treatment (positive control group); and groups 3 and 4 were intravenously administered either free URI or NSU-MAs at the same UCU dose of 2000 mU/kg, respectively. The blood samples of six mice in each group were collected from the eye socket at various time intervals (10, 30, 60, and 90 min), and plasma uric acid levels were measured using a clinically available assay kit (Nanjing Jiancheng Bioengineering Institute, Nanjing, China) after centrifugation (3000 rpm for 10 min) as previously described.[11]

The uric acid-lowering effects of NSU-MAs via subcutaneous administration were arranged as follows: group 5 (six rats per group) was a normal rat group (negative control group); group 6 was a hyperuricemia rat model group without treatment (positive control group); and groups 7 and 8 were subcutaneously administered either free URI or NSU-MAs at the same UCU dose of 2000 mU/kg, respectively.

Immunogenicity Test. Antisera against free URI and NSU-MAs in male SD rats were prepared as previously described.[14,16] Four groups of SD rats (six rats per group) were arranged as follows: group 1 was provided with saline water (negative control); group 2 was provided with ovalbumin (positive control); and groups 3 and 4 were provided with free URI and NSU-MA, respectively. The rats were intravenously boosted every week for 6 weeks with the corresponding antigen at the same dose of 500 μg/kg. The blood samples were collected at 24 h after each injection and subjected to centrifugation at 3500 rpm for 10 min. The profile of the obtained sera was determined using an ELISA, and the antibody versus time profile was depicted.[16] The blood samples were collected prior to the first injection and on day 14 after the last injection. The resulting sera were measured using an ELISA, and then the highest dilution ratio and antibody titers were obtained.[11] The ELISA was used to determine the level of anti-URI antibodies. Briefly, microtiter plates were coated with antigen and stored at 4 °C overnight. The plates were then rinsed three times with PBST solution. Next, 5% BSA blocking solutions were added to the wells for 1.5 h. The tested rat serum samples were diluted with 0.5% BSA and added to the plates. Then, the plates were incubated at 37 °C for 1 h and rinsed five times with PBST, followed by incubation with 100 μL of goat antirat IgG(H+L)/HRP. The wells were washed, the TMB color liquid was added to the wells and the plates were incubated for 10 min at 25 °C. The color reaction was halted by adding 2 mol/L of sulfuric acid. The absorbencies of the wells were determined at 450 nm. The anti-URI antibody titer was defined as the greatest dilution of the serum that resulted in an optical density 2.1 times higher than the negative control.

DOI: 10.1021/acsami.5b05758
ACS Appl. Mater. Interfaces 2015, 7, 20255−20263

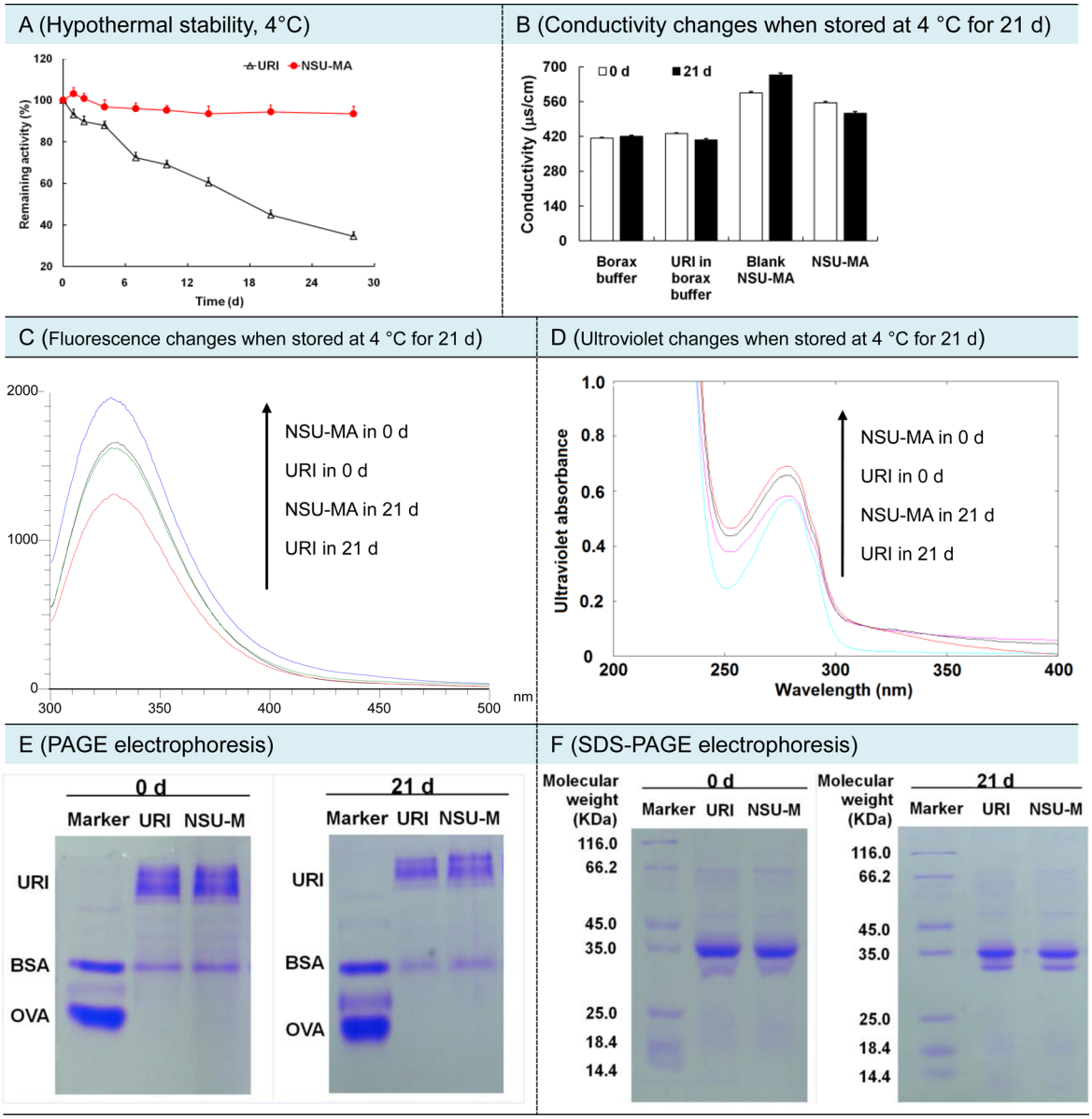

Figure 2. Effects of low temperature on the activity, electricity property, configuration and structure of NSU-MAs. (A) The URI activity, (B) conductivity, (C) fluorescence, (D) ultraviolet, and (E, F) electrophoresis changes of NSU-MAs when placed at 4 °C. The original activity of URI or NSU-MAs was taken as 100% in Figure A. The data were presented as mean ± standard deviation, $n = 3$. PAGE: Polyacrylamide gel electrophoresis. SDS-PAGE: Sodium dodecyl sulfate-polyacrylamide gel electrophoresis. BSA: Bovine serum albumin. OVA: Ovalbumin. The molecular weights of BSA and OVA were 66 kDa and 45 kDa, respectively.

Hemolysis Test. Four cuvettes containing 2.5 mL of 5% rabbit erythrocyte dispersion[17,18] were added to 0.5 mL of free URI plus 2 mL of saline water, 0.5 mL of NSU-MAs plus 2 mL of saline water, 2.5 mL of saline water (negative control), and 2.5 mL of distilled water (positive control). After vortexing, the mixtures were incubated at 37 °C for 1 h and imaged. These samples were then centrifuged at 3000 rpm for 10 min, and the supernatant were diluted with the same volume of pH 7.4 PBS, at which time the absorbance was recorded at 540 nm using a spectrophotometer (UV-2600, Shimadzu). The hemolysis rate was calculated as follows:

$$\text{hemolysis rate (\%)} = (\text{absorbance of sample} / \text{absorbance of positive control}) \times 100\%$$

Vascular Simulation. Vascular simulation of the ear vein in rabbits was performed as previously described.[19] Briefly, three groups of New Zealand rabbits (four rabbits per group) were arranged as follows: group 1 and 2 were intravenously administered free URI and NSU-MAs into the left ears, respectively; group 3 was administered penicillin (positive control) into the left ear; and groups 1−3 were administered saline water into the right ears (negative control). The rabbits were intravenously injected everyday for 5 consecutive days. The rabbits were restored over 3 h after depilation of the injection site and surrounding tissue, followed by sterilization with 75% alcohol. After local anesthesia with pentobarbital, the tissues were cut approximately 5 cm along the injection site to the centripetal end, washed with saline water, and fixed with 10% formaldehyde for 2 d. The tissues were embedded in paraffin, sliced, and stained with hematoxylin and eosin. The pathology slides were examined under a Nikon Eclipse Ti−S inverted microscope.

Statistical Analysis. All of the data are shown as the mean ± standard deviation unless noted. The Student's paired t test was used to calculate significant differences. Statistical significance was established at $P < 0.05$. Pharmacokinetic and bioequivalence analyses were conducted using DAS software (Mathematical Pharmacology Professional Committee of China, Shanghai, China).

DOI: 10.1021/acsami.5b05758
ACS Appl. Mater. Interfaces 2015, 7, 20255−20263

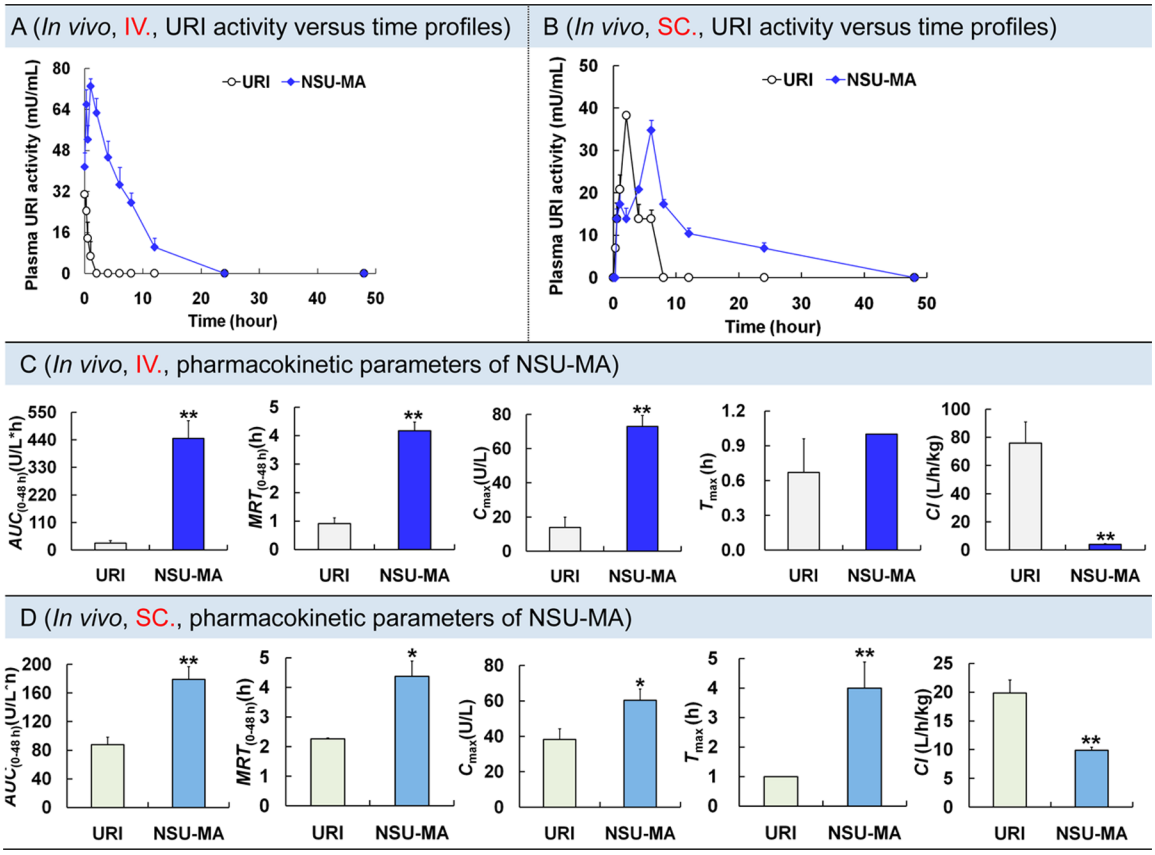

Figure 3. In vivo kinetic characteristics of URI and NSU-MAs. Plasma URI activity versus time profiles after (A) intravenous and (B) subcutaneous injections of URI and NSU-MAs at the same dose (2000 mU/kg of URI). The data were shown as mean ± SD n = 6 rats per group. Main pharmacokinetic parameters of URI and NSU-MAs after (C) intravenous and (D) subcutaneous injection. *P < 0.05 or **P < 0.01 indicate significant differences between NSU-MAs and URI. Abbreviations: AUC, area under the plasma concentration−time curve; MRT, mean residence time; C_{max}, maximum concentration; T_{max}, peak time; Cl, clearance rate.

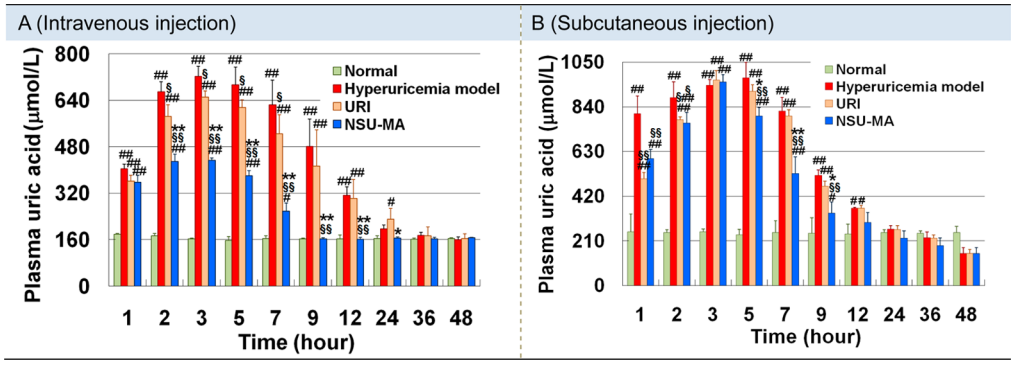

Figure 4. Uric acid-lowering effects of NSU-MAs on the hyperuricemia rats. Plasma uric acid concentration versus time profiles after (A) intravenous or (B) subcutaneous injections of NSU-MAs. The data were shown as mean ± SD n = 6 mice per group. # (or ##) indicated significant differences (P < 0.05 or P < 0.01) compared with normal group; §(or §§) indicated significant differences (P < 0.05 or P < 0.01) compared with hyperuricemia model group; *(or **) indicated significant differences (P < 0.05 or P < 0.01) compared with free URI group.

RESULTS AND DISCUSSION

Preparation and Characterization of NSU-MA. NSU-MAs were successfully prepared through a modified multiple emulsion solvent evaporation method as shown in Figure S1A. Under the confocal laser microscope, NSU-MAs were assembled by many smaller and round nanosomes (Figure 1A and 1B). When incubated at a physiological pH of 7.4, the NSU-MAs gradually and physically decomposed in two patterns: squeezing out smaller round nanosomal assemblies (Figure 1C) or breaking into smaller irregular nanosomal assemblies (Figure 1D). The factors that could influence the decomposition patterns include the temperature, the media pH, the amount of NSU-MAs, and the URI concentration. More efforts are necessary before we can identify the critical factors in determining the decomposition patterns. The multilayered colloidal liquid aphrons composed of many droplets were more stable than a single droplet, and the high stability of the colloidal aphrons was due to thin shells surrounding the cores.[20] It is reasonable to deduce that the nanosomal assemblies comprised of many nanosomes had much higher

DOI: 10.1021/acsami.5b05758
ACS Appl. Mater. Interfaces 2015, 7, 20255−20263

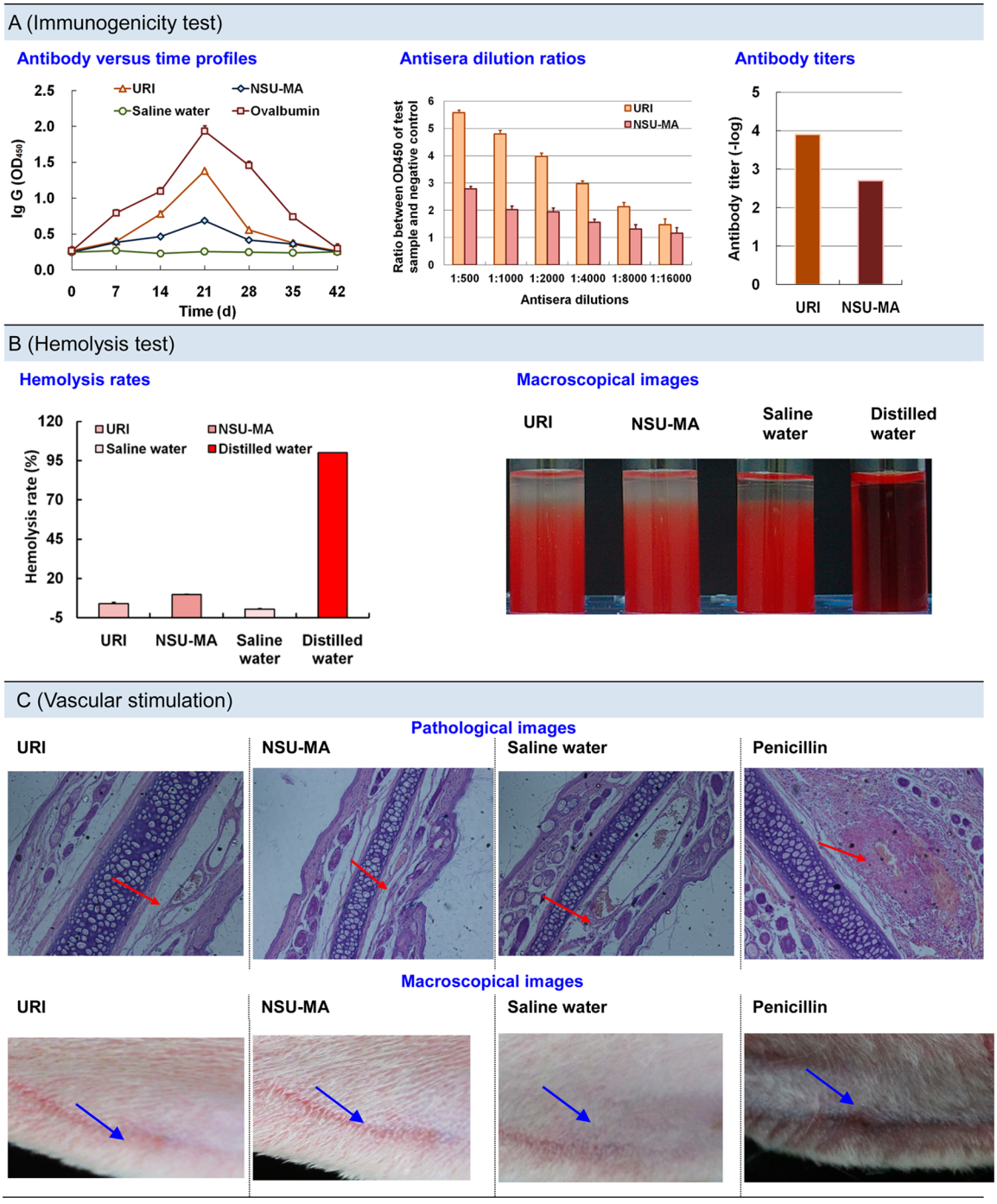

Figure 5. Preliminary safety evaluation of NSU-MAs. (A) Immunogenicity, (B) hemolysis, and (C) vascular stimulation of NSU-MAs. The data were shown as mean ± SD, n = 3. Saline water was taken as the negative control in all tests, while the ovalbumin, distilled water and penicillin were separately taken as the positive control in immunogenicity, hemolysis, and vascular stimulation tests.

stability than a single nanosome in a similar manner to colloidal liquid aphrons, and the small size of the nanosome created a system with a high interface area that can be pumped like water without collapsing. NSU-MAs showed a spherical morphology with a diameter of 22.56 ± 1.70 μm (Figure S1B) and a zeta potential of −41.81 ± 6.59 mV (Figure S1C) (n = 3). The high electric potential value suggests the existence of an energy efficient barrier for stabilizing the microvesicles. NSU-MAs produced higher electrical conductivity compared to free URI (Figure 2B), indicating the higher electricity situations of the microenvironment of URI in NSU-MAs. The lipid vesicle loading was favorable toward the high electricity situations of URI. The encapsulation efficiency was 63.75 ± 3.65% (n = 3) as determined by a centrifugation method for separation of the free URI.[4] The encapsulation efficiency of enzyme delivery vesicles usually ranged from 10% to 67%.[10]

There are existing interactions between enzymes and lipid membranes.[21] To demonstrate the native state of URI in NSU-MAs, we investigated the interaction between URI and the vesicle membrane using a FITC fluorescence method.[4] Figure S1D shows that the fluorescence intensity of URI-FITC decreased when URI was incubated with blank NSU-MAs in

DOI: 10.1021/acsami.5b05758
ACS Appl. Mater. Interfaces 2015, 7, 20255−20263

advance, which indicated a competitive interaction of URI and FITC with the zwitterionic lipid membrane interface through electrostatic and hydrophobic effects.[4,22,23] We deduce that URI exists in the NSU-MAs in three ways: (1) URI is attached to the outer surface of NSU-MAs, which in clinical practice may enable rapid therapeutic efficacy for patients in a similar manner as superoxide dismutase (SOD) does. SOD covalently attaches to the outer surface of enzymosomes, which accelerated its therapeutic activity compared to both free SOD and SOD encapsulated inside enzymosomes.[24] (2) URI is attached to the inner surface of NSU-MAs; and (3) URI is simply trapped inside NSU-MAs without attaching to the membrane. The sustained enzyme activity confirmed by *in vivo* kinetic experiments may ascribe to the last two URI types. The NSU-MA membranes have two functions: to restrict URI to the internal liquid environment consisting of a buffer with an alkaline pH beneficial for catalytic reactions and to separate the unstable large molecular URI from external environments, and enhance its hypothermal, thermal, acid−base and proteolytic stabilities over free URI.

Effects of Temperature on the Activity of NSU-MAs. Temperature has a considerable influence on enzyme activity. The URI in the NSU-MAs exerted maximum catalyzing activity at 40 °C (Figure S2). The maximum activity of the NSU-MAs was approximately 30% higher than that of free URI. Figure 2B and Figure S3A show that NSU-MAs had significantly increased hypothermal (4 °C) and thermal (55 °C) stabilities compared to free URI. When subjected to 4 °C for 28 d, NSU-MA maintained approximately 94% activity, whereas the free URI lost 10% and 50% of its maximum activity at 2 and 18 d, respectively. To discover the possible reasons for the high stability of NSU-MAs, we investigated the effects of low temperature on the electrical characteristics, conformational changes, and molecular and chemical structure changes by measuring conductivities; fluorescence spectroscopy, ultraviolet spectroscopy and polyacrylamide gel electrophoresis (PAGE); and sodium dodecyl sulfate (SDS)-PAGE, respectively.[25] Electrical conductivity of NSU-MAs refers to the current-induced electric field at a point in the semiconductor divided by the current density.[26] When placed at 4 °C for 21 d, the conductivity of the NSU-MAs was approximately 26.50% higher than the free URI, compared to 28.55% higher electrical conductivity than free URI at the beginning (Figure 2B). The electrical conductivities of NSU-MAs and free URI decreased approximately 7.44% and 5.94%, respectively. These results indicated that the lipid loading and not cold storage caused the observed changes of the electrical situation of the URI microenvironment. The location of the hydrophobic moiety of URI is essential to catalyze the reaction and is relevance to its catalytic efficiency.[27] Fluorescence or ultraviolet intensity and wavelength reflect the conformational changes of proteins.[15] A decrease in either the fluorescence intensities or ultraviolet absorption of the NSU-MAs at their maximal wavelengths (Figure 2C and 2D) suggested the movement of tryptophan groups of URI from the inner hydrophobic cores to outer hydrophilic surfaces after cold storage, thus affecting the URI catalytic activity. To demonstrate the decomposition situation of URI, we conducted native PAGE.[5,6] URI in the NSU-MAs was detected primarily in its tetrameric (140 kDa) form, and only a small portion existed as adimer (70 kDa) after cold storage (Figure 2E). The lipid vesicle loading is favorable to keep the tetramer form of URI intact. Next, we conducted SDS-PAGE[25] to investigate the molecular and chemical structure changes of URI. After cold storage, URI in the NSU-MAs had similar bands (35 kDa) as those prior to cold storage (Figure 2F), which indicates that there were no obvious changes in the molecular and chemical structures of URI loaded with NSU-MAs. When subjected to 55 °C, NSU-MAs maintained over 90% activity after 5 h, whereas free URI lost 10% and 50% activity at 0.5 and 4 h, respectively. The thermal inactivation of URI was related to conformational changes, such as the loss of its helical structure and tertiary structure,[4,28] and subsequently, the detected URI fluorescence changes reflect these conformational changes. As depicted in Figure S3B, the fluorescence intensity of free URI was markedly decreased when incubated at 55 °C for 3 h, indicating that the microenvironment of the aromatic groups such as the tryptophan irreversibly became more hydrophobic, as analyzed by Tan et al.[4] However, some enzymatic conformational changes can induce the exposure of hydrophobic clusters to the aqueous media, causing these proteins to become more hydrophilic.[29] In the case of NSU-MAs, the increased fluorescence intensity may ascribe to the enhanced hydrophilic microenvironment of the URI aromatic groups, which varied due to the following synthetic effects: (1) the attachment of native URI molecules to the inner or outer membrane interfaces of NSU-MAs, as suggested by Figure S1D; (2) the conjugation of denatured URI molecules to the membranes; and (3) either native or denatured URI enclosed inside membranes. Considering the higher activities of NSU-MAs than those of URI and the microenvironmental differences between them, the interaction of URI and the membrane might have the most predominant influence on the thermal stability of NSU-MAs.

Effects of Acidity and Alkalinity on the Activity of NSU-MAs. Acidity-alkalinity (pH) also has a pronounced influence on URI activity.[30] The catalyzing reaction of NSU-MAs was the fastest at pH 8.0 (Figure S4A). The maximal activity of NSU-MAs was approximately 46% higher than that of free URI. Figure S4B showed that the remaining activity of NSU-MAs was higher than the free URI at every identified pH, including at physiological pH and the optimal pH of URI. Furthermore, the remaining activity of either NSU-MAs or URI was higher in an alkaline environment compared to an acidic situation. The NSU-MA membrane separated URI from the external environment, which enhanced its pH stability over URI.

Effects of Proteolytic Enzyme on the Activity of NSU-MAs. We then sought to verify that NSU-MAs facilitated the remaining URI activity when treated with a proteolytic enzyme such as trypsin. The length of time in which 90% and 50% of URI activity was sustained in NSU-MAs was approximately 4 times and 2 times that of free URI (Figure S5). These data clearly showed that URI was stabilized by loading with lipid NSU-MA vesicles.

Comprehensive Kinetic Features of NSU-MA. To demonstrate the comprehensive kinetic features of NSU-MAs, we determined its kinetic parameters such as the Michaelis constant (K_m) in vitro and the area under the plasma concentration−time curve (AUC) in vivo. Generally, the lower the K_m, the higher the affinity between an enzyme and its substrate. The apparent K_m value of the NSU-MAs was slightly lower than that of free URI (Figure S6), and it was a synthesized exhibition of the affinity properties of membrane-entrapped and membrane-conjugated URI. Catalysis of the NSU-MAs might be either homogeneous or heterogeneous. When rats were intravenously administered URI, the NSU-MAs

DOI: 10.1021/acsami.5b05758
ACS Appl. Mater. Interfaces 2015, 7, 20255−20263

were able to modulate the pharmacokinetic behavior of URI (Figure 3A). As illustrated in Figure 3C, the maximum activity of NSU-MAs was 5.25 times that of free URI. It took 1.49 times longer for NSU-MAs to achieve its peak activity compared to free URI; however, the NSU-MAs maintained elevated URI activity levels for over 12 h with a clearance rate of only 5% that of free URI. All of these results significantly contributed to the increased bioavailability of NSU-MAs compared to free URI. Similarly, after subcutaneous injection, the NSU-MAs exhibited a prolonged plasma profile and altered the kinetic parameters compared to free URI (Figure 3B and 3D). As shown in Table S1, the NSU-MAs and free URI were not bioequivalent based on the stipulated bioequivalence criteria.[13,31] The NSU-MAs had higher bioavailability, stronger catalytic activity and longer peak time of activity.

Uric Acid Lowering Efficacy of NSU-MAs. To evaluate the efficacy of NSU-MAs, a rat model of hyperuricemia was used for in vivo assessments.[11,14,32] Clinically, URI is usually administered intravenously. After intravenous administration of NSU-MAs, the plasma uric acid levels of the hyperuricemia rats significantly decreased. It took only 20% of the time for NSU-MAs to lower the plasma uric acid concentration from the same elevated levels to physiologically normal levels compared to free URI (Figure 4A). When injected subcutaneously,[33] NSU-MAs also achieved improved uric acid-lowering effects compared to free URI (Figure 4B). Unsurprisingly, intravenous administration of NSU-MAs induced a more effective therapeutic response compared to subcutaneous administration. NSU-MAs had better therapeutic effects than free URI, which was the synthetic result of several factors: NSU-MAs had higher catalyzing activity than free URI at physiological pH and temperature; NSU-MAs maintained higher activity in the circulatory system due to its improved stability at varying temperatures, acidity-alkalinity systems and proteolytic environments; and NSU-MAs had longer acting time in vivo due to its decreased clearance rate. Essentially, NSU-MAs ensured that over a longer period, URI was delivered in favorable microenvironments where catalytic reactions occurred.

Immunogenicity of NSU-MAs. The side effects of free URI, such as hypersensitivity and anaphylaxis, are closely related to its high immunogenicity.[34] NSU-MAs are expected to have decreased immunogenicity by either entrapping or conjugating URI with biodegradable pharmaceutical excipients. We calculated an antibody versus time profile[16] and the antibody titer[14] (Figure 5A) using the enzyme-linked immune sorbent assay method. Free URI had high immunogenicity, whereas the maximum antibody levels produced by NSU-MAs after 21 d was approximately 50% that of free URI. It has been suggested that NSU-MAs had lower immunogenicity than free URI. Based on the method of ratio analysis, the greatest dilution obtained for NSU-MAs (1:8000) was much lower than that for free URI (1:500), and the antibody titer of the NSU-MAs was obviously lower than free URI. This supports the notion that NSU-MAs induce a weaker immune response compared to free URI.

Hemolysis and Vascular Stimulation. To evaluate the systemic and local toxicities, we determined hemolysis and vascular stimulation.[17,18] NSU-MAs have a low hemolysis rate (<10%) compared to the positive control (Figure 5B). When NSU-MAs were injected, there was neither obvious congestion and thrombosis nor obvious inflammatory cell infiltration in the vessel wall and its surrounding regions (Figure 5C). Microscopic and macroscopic images revealed inconspicuous pathological changes induced by NSU-MAs. Thus, NSU-MAs is suitable for injection.

CONCLUSION

To provide effective and safe delivery of therapeutic enzymes in hyperuricemia therapy, we have rationally fabricated a uricase loading nanosomal microassembly (NSU-MA) that possesses a number of characteristics as a superior enzyme delivery system. To verify the merits of this delivery system, the changes of catalytic activity under different temperatures, acidity-alkalinity environments and proteolytic enzymes were first investigated, followed by the determination of the comprehensive kinetic features, including efficacy, immunogenicity, hemolysis and vascular stimulation. We demonstrated that compared to free URI, the nanosomal microassembly exhibited much higher catalytic activity at physiological pH and temperature; the catalytic activities remained higher when subjected to high or low temperature, a wide pH range (6.5−9.5) and trypsin; and NSU-MAs displayed increased circulation time, raised bioavailability, and enhanced uric acid-lowering efficacy, while simultaneously decreasing the immunogenicity. A low hemolysis rate and no obvious vascular stimulation were observed upon injection of NSU-MAs into rabbits. We also describe the possible conformational changes occurred in NSU-MAs that result in favorable reactions. It was rationally deduced that, by either entrapping or conjugating URI with nanosomal microassemblies, the URI in NSU-MAs was suited for a favorable microenvironment where catalytic reactions occurred over a longer period compared to free URI (Figure S7). Because enzyme therapy is more effective than the traditional chemotherapy for the treatment of hyperuricemia, overcoming delivery obstacles by using nanosomal microassemblies can provide a superior enzyme delivery system for the delivery of effective and safe therapy against hyperuricemia.

ASSOCIATED CONTENT

Supporting Information

The Supporting Information is available free of charge on the ACS Publications website at DOI: 10.1021/acsami.5b05758.

Preparation, characteristics, and bioequivalence evaluation of NSU-MAs, schematic illustration of the preparation, optimal temperature of NSU-MAs, thermal stability of NSU-MAs, effects of acidity-alkalinity, proteolytic stability of NSU-MAs, enzymatic kinetics of NSU-MAs, schematic illustration of how NSU-MAs work, and bioequivalence evaluation of NSU-MAs (PDF)

AUTHOR INFORMATION

Corresponding Author

*E-mail: zjqrae01@163.com.

Author Contributions

#H.X., Y.Z., Q.Z., D.H., and S.W. contributed equally to this work.

Notes

The authors declare no competing financial interest.

ACKNOWLEDGMENTS

This research was partially supported by grants from National Natural Science Foundation of China (No 30973645) and

DOI: 10.1021/acsami.5b05758
ACS Appl. Mater. Interfaces 2015, 7, 20255−20263

Chongqing Education Committee Fund (Excellent university personnel financial aid plan, KJ120321).

REFERENCES

(1) Liu, H.; Zhang, X. M.; Wang, Y. L.; Liu, B. C. Prevalence of Hyperuricemia Among Chinese Adults: A National Cross-sectional Survey Using Multistage, Stratified Sampling. *J. Nephrol.* **2014**, *27*, 653.

(2) Grassi, D.; Desideri, G.; Di Giacomantonio, A. V.; Di Giosia, P.; Ferri, C. Hyperuricemia and Cardiovascular Risk. *High Blood Pressure Cardiovasc. Prev.* **2014**, *21*, 235−242.

(3) Beedkar, S. D.; Khobragade, C. N.; Bodade, R. G.; Vinchurkar, A. S. Comparative Structural Modeling and Docking Studies of Uricase: Possible Implication in Enzyme Supplementation Therapy for Hyperuricemic Disorders. *Comput. Biol. Med.* **2012**, *42*, 657−666.

(4) Tan, Q. Y.; Wang, N.; Yang, H.; Zhang, L. K.; Liu, S.; Chen, L.; Liu, J.; Zhang, L.; Hu, N. N.; Zhao, C. J.; Zhang, J. Q. Characterization, Stabilization and Sctivity of Uricase Loaded in Lipid Vesicles. *Int. J. Pharm.* **2010**, *384*, 165−172.

(5) Feng, J.; Liu, H.; Yang, X.; Gao, A.; Liao, J.; Feng, L.; Pu, J.; Xie, Y.; Long, G.; Li, Y.; Liao, F. Comparison of Activity Indexes for Recognizing Enzyme Mutants of Higher Activity with Uricase as Model. *Chem. Cent. J.* **2013**, *7*, 69.

(6) Lopez-Olivo, M. A.; Pratt, G.; Palla, S. L.; Salahudeen, A. Rasburicase in Tumor Lysis Syndrome of the Adult: a Systematic Review and Meta-analysis. *Am. J. Kidney Dis.* **2013**, *62*, 481−492.

(7) George, R. L., Jr; Sundy, J. S. Pegloticase for Treating Refractory Chronic Gout. *Drugs Today (Barc.)* **2012**, *48*, 441−449.

(8) Zhang, C.; Yang, X. L.; Yuan, Y. H.; Pu, J.; Liao, F. Site-specific PEGylation of Therapeutic Proteins via Optimization of both Accessible Reactive Amino Acid Residues and PEG Derivatives. *BioDrugs* **2012**, *26*, 209−215.

(9) U.S. Food and Drug Administration. FDA website, 2010. http://www.accessdata.fda.gov/drugsatfda_docs/label/2010/125293s0000lbl.pdf.

(10) Tan, Q. Y.; Wang, N.; Yang, H.; Chen, L.; Xiong, H. R.; Zhang, L. K.; Liu, J.; Zhao, C. J.; Zhang, J. Q. Preparation and Characterization of Lipid Vesicles Containing Rricase. *Drug Delivery* **2010**, *17*, 28−37.

(11) Tan, Q.; Zhang, J.; Wang, N.; Li, X.; Xiong, H.; Teng, Y.; He, D.; Wu, J.; Zhao, C.; Yin, H.; Zhang, L. Uricase from Bacillus Fastidious Loaded in Alkaline Enzymosomes: Enhanced Biochemical and Pharmacological Characteristics in Hypouricemic Rats. *Eur. J. Pharm. Biopharm.* **2012**, *82*, 43−48.

(12) Lu, B.; Zhang, J.; Yang, H. Non Phospholipid Vesicles of Carboplatin for Lung Targeting. *Drug Delivery* **2003**, *10*, 87−94.

(13) Zhong, M.; Feng, Y.; Liao, H.; Hu, X.; Wan, S.; Zhu, B.; Zhang, M.; Xiong, H.; Zhou, Y.; Zhang, J. Azithromycin Cationic Non-lecithoid Nano/microparticles Improve Bioavailability and Targeting Efficiency. *Pharm. Res.* **2014**, *31*, 2857−2867.

(14) Tan, Q. Y.; Zhang, J.; Wang, N.; Yang, H.; Li, X.; Xiong, H. R.; Wu, J. Y.; Zhao, C. J.; Wang, H.; Yin, H. F. Improved Biological Properties and Hypouricaemic Effects of Uricase from Candida utilis Loaded in Novel Alkaline Enzymosomes. *Int. J. Nanomed.* **2012**, *7*, 3929−3938.

(15) Qiu, Y. Z.; Huang, Z. H.; Song, F. J. Enzymatic Activity Enhancement of Non-covalent Modified Superoxide Dismutase and Molecular Docking Analysis. *Molecules* **2012**, *17*, 3945−3956.

(16) Zhang, C.; Fan, K.; Ma, X.; Wei, D. Impact of Large Aggregated Uricases and PEG Diol on Accelerated Blood Clearance of PEGylated Canine Uricase. *PLoS One* **2012**, *7*, e39659.

(17) Utreja, P.; Jain, S.; Yadav, S.; Khandhuja, K. L.; Tiwary, A. K. Efficacy and Toxicological Studies of Cremophor EL Free Alternative Paclitaxel Formulation. *Curr. Drug Saf.* **2011**, *6*, 329−338.

(18) Zhang, J.; Zhang, Z. R.; Yang, H.; Tan, Q. Y.; Qin, S. R.; Qiu, X. L. Lyophilized Paclitaxel Magnetoliposomes as a Potential Drug Delivery System for Breast Carcinoma via Parenteral Administration: in Vitro and in Vivo Studies. *Pharm. Res.* **2005**, *22*, 573−583.

(19) Jin, Y.; Wang, P.; Wang, X. W.; Liu, Y. P. Comparison and suggestion of vascular stimulation tests in drug safety evaluation between China and Japan. *Chinese Journal of New Drugs* **2012**, *21*, 1328−1331 Written in Chinese.

(20) Molaei, A.; Waters, K. E. Aphron applications - A review of recent and current research. *Adv. Colloid Interface Sci.* **2015**, *216*, 36−54.

(21) Martfeld, A. N.; Rajagopalan, V.; Greathouse, D. V.; Koeppe, R. E. Dynamic Regulation of Lipid-protein Interactions. *Biochim. Biophys. Acta, Biomembr.* **2015**, No. S0005-2736(15)00029-2.18481849.

(22) Roberts, S. A.; Kellaway, I. W.; Taylor, K. M.; Warburton, B.; Peters, K. Combined Surface Pressure-interfacial Shear Rheology Studies of the Interaction of Proteins with Spread Phospholipid Monolayers at the Air-water Interface. *Int. J. Pharm.* **2005**, *300*, 48−55.

(23) Yoshimoto, M. Stabilization of Enzymes through Encapsulation in Liposomes. *Methods Mol. Biol.* **2011**, *679*, 9−18.

(24) Corvo, M. L.; Marinho, H. S.; Marcelino, P.; Lopes, R. M.; Vale, C. A.; Marques, C. R.; Martins, L. C.; Laverman, P.; Storm, G.; Martins, M. B. Superoxide Dismutase Enzymosomes: Carrier Capacity Optimization, in Vivo Behaviour and Therapeutic Activity. *Pharm. Res.* **2015**, *32*, 91−102.

(25) Liu, X.; Wen, M.; Li, J.; Zhai, F.; Ruan, J.; Zhang, L.; Li, S. High-yield Expression, Purification, Characterization, and Structure Determination of Tag-free Candida utilis Uricase. *Appl. Microbiol. Biotechnol.* **2011**, *92*, 529−537.

(26) Hu, J.; Chen, D.; Jiang, R.; Tan, Q.; Zhu, B.; Zhang, J. Improved Absorption and in Vivo Kinetic Characteristics of Nanoemulsions Containing Evodiamine-phospholipid Nanocomplex. *Int. J. Nanomed.* **2014**, *9*, 4411−4420.

(27) Colloc'h, N.; Prangé, T. Functional Relevance of the Internal Hydrophobic Cavity of Urate Oxidase. *FEBS Lett.* **2014**, *588*, 1715−1719.

(28) Caves, M. S.; Derham, B. K.; Jezek, J.; Freedman, R. B. Thermal Inactivation of Uricase (Urate Oxidase): Mechanism and Effects of Additives. *Biochemistry* **2013**, *52*, 497−507.

(29) Mei, G.; Di Venere, A.; Buganza, M.; Vecchini, P.; Rosato, N.; Finazszi-Agró, A. Role of Quaternary Structure in the Stability of Dimeric Proteins: the Case of Ascorbate Oxidase. *Biochemistry* **1997**, *36*, 10917−10922.

(30) Huang, Y.; Chen, Y.; Yang, X.; Zhao, H.; Hu, X.; Pu, J.; Liao, J.; Long, G.; Liao, F. Optimization of pH Values to Formulate the Bireagent Kit for Serum Uric Acid Assay. *Biotechnol. Appl. Biochem.* **2015**, *62*, 137.

(31) Hu, J.; Sun, L.; Zhao, D.; Zhang, L.; Ye, M.; Tan, Q.; Fang, C.; Wang, H.; Zhang, J. Supermolecular Evodiamine Loaded Water-in-oil nanoemulsions: Enhanced Physicochemical and Biological Characteristics. *Eur. J. Pharm. Biopharm.* **2014**, *88*, 556−564.

(32) Liu, L. M.; Cheng, S. F.; Shieh, P. C.; Lee, J. C.; Chen, J. J.; Ho, C. T.; Kuo, S. C.; Kuo, D. H.; Huang, L. J.; Way, T. D. The Methanol Extract of Euonymus Laxiflorus, Rubia Ianceolata and Gardenia Jasminoides Inhibits Xanthine Oxidase and Reduce Serum Rric Acid Level in Rats. *Food Chem. Toxicol.* **2014**, *70*, 179−184.

(33) Geraths, C.; Daoud-El Baba, M.; Charpin-El Hamri, G.; Weber, W. A Biohybrid Hydrogel for the Urate-responsive Release of Urate Oxidase. *J. Controlled Release* **2013**, *171*, 57−62.

(34) Yang, X.; Yuan, Y.; Zhan, C. G.; Liao, F. Uricases as Therapeutic Agents to Treat Refractory Gout: Current States and Future Directions. *Drug Dev. Res.* **2012**, *73*, 66−72.

DOI: 10.1021/acsami.5b05758
ACS Appl. Mater. Interfaces 2015, 7, 20255−20263